

Direct Measurement Sensor of the Boundary Shear Stress in Fluid Flow

Mircea Badescu, Xiaoqi Bao, Yoseph Bar-Cohen, Zensheu Chang, Kornel Kerenyi*, Shyh-Shiuh Lih, Stewart Sherrit, Brian P. Trease, and Scott Widholm

Jet Propulsion Laboratory, California Institute of Technology, (MS 67-119), 4800 Oak Grove Drive, Pasadena, CA 91109-8099, Phone 818-393-5700, Fax 818-393-2879, Mircea.Badescu@jpl.nasa.gov
web: <http://ndea.jpl.nasa.gov>

* Federal Highway Administration, TFHRC, Office of Infrastructure R&D, T111, 6300, Georgetown Pike, McLean, VA 22101

ABSTRACT

The flow fields and boundary erosion that are associated with scour at bridge piers are very complex. Direct measurement of the boundary shear stress and boundary pressure fluctuations in experimental scour research has always been a challenge and high spatial resolution and fidelity have been almost impossible. Most researchers have applied an indirect process to determine shear stress using precise measured velocity profiles. Laser Doppler Anemometry and Particle Image Velocimetry are common techniques used to accurately measure velocity profiles. These methods are based on theoretical assumptions to estimate boundary shear stress. In addition, available turbulence models cannot very well account for the effect of bed roughness which is fundamentally important for any CFD simulation. The authors have taken on the challenge to advance the magnitude level to which direct measurements of the shear stress in water flow can be performed. This paper covered the challenges and the efforts to develop a higher accuracy and small spatial resolution sensor. Also, preliminary sensor designs and test results are presented.

KEYWORDS: Sensor, shear stress, fluid flow.

1.0 INTRODUCTION

The flow fields and boundary erosion that are associated with scour at bridge piers are very complex. In particular, scour development is complicated by the important effects of large scale turbulence structures (macro-turbulence) that markedly characterize pier flow fields. The role that such turbulence structures play in scour has only been partially appreciated. It is a role that needs to be very well-understood when investigating scour at bridge piers. Turbulence structures, together with local flow convergence / contractions around the fronts and flanks of piers, or between piles of complex pier configurations, are erosive flow mechanisms of primary importance. The interactions of macro-turbulence structures with themselves and converging flows are of key significance in illuminating how pier geometry affects sediment entrainment and thereby scour morphology and maximum scour depth. The measurement of shear stress has applications in many other problems including the performance and transportation vehicles and surface flow characterization [Naughton and Sheplak, 2002].

Direct measurement boundary shear stress and boundary pressure fluctuations in experimental scour research has always been a challenge and almost impossible. This method measures the displacement of a plate due to shear force developed in contact with a flow. Akasofu and Neuman [Akasofu, 1991] used the change of the capacitance of a capacitor bridge to measure the deformation of a silicon gel layer due to shear force. This is relatively simple solution, small scale and easy to seal but the sensitivity, electric shielding and material stability raise issues regarding its use. Roche et al [1996] developed a sensor based on piezoelectric biomorphs with a plate at the top. It is more applicable to AC shear stress rather than a DC shear stress and so it is difficult to work with at very low frequency.

Most researchers have applied an indirect process to determine shear stress using precise measured velocity profiles. Laser Doppler Anemometry and Particle Image Velocimetry are common techniques used to accurately measure velocity profiles. These methods are based on theoretical assumptions to estimate boundary shear stress. In addition, available turbulence models cannot very well account for the effect of bed roughness which is fundamentally important for any CFD simulation. Yucel and Graf [1975] developed a method to determine the shear force in a sand-water mixture flow by measuring the voltage required to maintain a flush-mounting hot-film at constant temperature. Qu et al [2008] determined the shear force by measuring the resistance of a carbon nanotube. Tunga et al [2007] used a similar

method and a sensor based on laterally aligned carbon nanotubes. Große et al [2006] used elastomeric cylindrical pillars with a diameter of a few microns and a high speed CCD camera to measure pillar's tip deflection.

A mechanical shear sensor device that was developed by the TFHRC Hydraulics Research team to measure wall shear stress directly has several limitations. One major trade off is that the sensor is limited to measure point shear stresses only. The sensor plate has to be perfectly aligned horizontally with the channel bed and cannot be used to measure shear stress in preformed scour holes. Therefore, there is a need to research a sensing system that can measure instantaneous areal boundary shear stresses and pressure fields for small scale bridge scour experiments. It is desired that the sensing system has the flexibility to measure the change in shear-stress and pressure when the scour hole forms. The development of such a sensing system is the objective of this proposed task.

2.0 Sensor design and structural analysis

Two flexure configurations were initially selected for the 10mm scale sensor: a 3D version and a 2D version. The 3D version flexure would allow a plate to rotate about an axis defined by three sets of flexures (see **Figure 1**). The plate is mounted on a beam that passes through this axis and extends on the other side of the axis where it has a free end. An encoder or capacitor sensor would read the displacement of the free end of the beam and based on the flexure stiffness, one can determine the shear force on the sensor plate. This configuration would use the horizontal blade to separate the test media from the encoder/capacitor but would present significant manufacturing and packaging challenges.

The 2-d version would allow a plate exposed to the flow to slide horizontally by being attached to the base thru a set of bending blades (see **Figure 2**). An encoder would read the displacement of this plate by attaching a tape scale underneath the plate. The blades need to be designed to have a low bending stiffness in the flow direction and high stiffness in all other directions. Additionally, the plate mounting needs to allow separation of the encoder read head from the test media.

After assessing the capabilities and challenges, the 2D flexure configuration was selected for further development due to easier fabrication and potential of further integration in an sensor array structure.

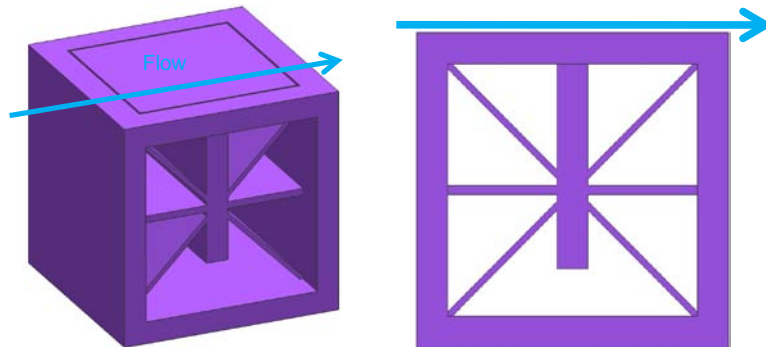


Figure 1: 3D rotary design configuration

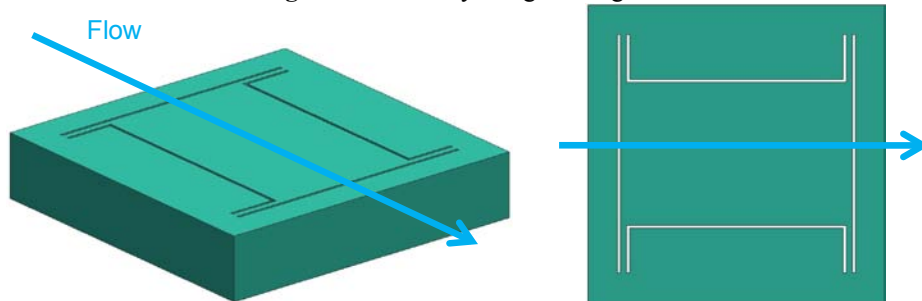


Figure 2: 2D floating plate design configuration

3.0 Sensor fabrication, instrumentation and test results

Using an EDM process a floating plate prototype was fabricated. The floating plate size was increased to 14x14mm to ease the handling and testing process. The effective area of the floating plate and the configuration and size of the blades were maintained the same as used in analysis. The blades configuration was selected such that it has low flow direction

stiffness and still maintaining a high modal frequency. The modal analysis showed a first resonant frequency of 487 Hz and a linear stiffness in the flow direction of 450N/m. The stress analysis showed a stress level of two orders of magnitude smaller than the maximum stress allowed for the selected material. A further improvement in the floating plate design was limited by the manufacturing process, i.e. the minimum gap between blades and the minimum blade thickness. **Figure 3** shows a rendering of the sensor plate design with a finite element analysis. The sensor mounting plate was later modified to reduce the distance between the scale and read head recommended by the manufacturer (**Figure 4**).

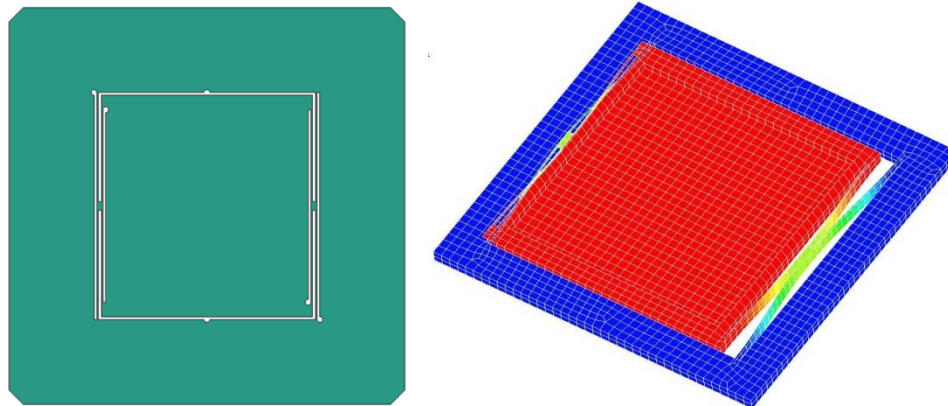


Figure 3: Sensor plate design and analysis.

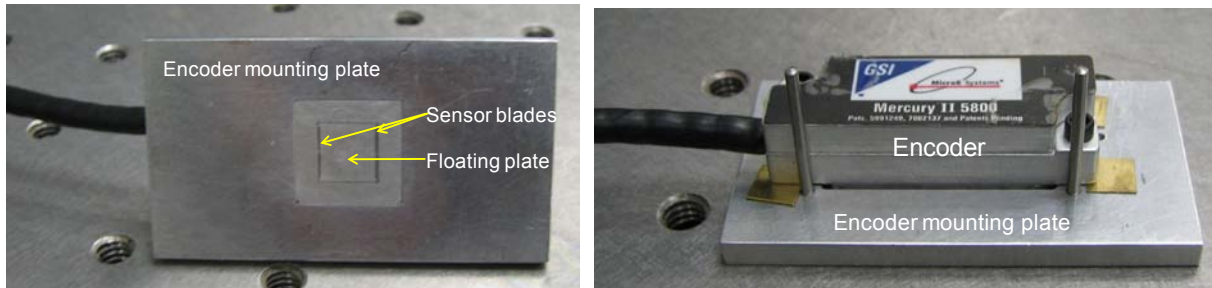


Figure 4: Sensor mounted assembly top (left) and bottom (right) views

4.0 Encoder performance in air and thru a water layer

We verified the encoder performance against the performance of the interferometer. The encoder read head and scale were mounted on a linear stage and the motion of this stage was controlled by a PST stack. The interferometer read head and the linear stage were mounted on a optical table without any additional vibration isolation measures or temperature control. The interferometer and the encoder were used to produce position data. The goal of this test was to determine the accuracy of the encoder by comparing its data with the interferometer output. Various methods (cross correlation, interpolation, center matching and scaling) were used to reduce the difference between the two readings. For the readings two sets of experiments were performed. In the first set in the gap between the encoder read head and encoder scale was air and the distance was maintained at 0.9mm and this set of experiments is referred as the "thru-air" experiments. In the second set in the gap was introduced a layer of water and it is referred as "thru-water" experiments, where the gap size was reduced to obtain the same power level for the encoder read head signal as in the "thru-air" test.

The data from the encoder and interferometer was originally not in phase with each other, resulting in significant differences. A cross correlation scheme was developed to match the two measurements in time domain via calculated time shift. Then the amplitude for the interferometer data was scaled and data shifted to reduce the root mean square errors. An intuitive way of scaling the amplitude would be matching the greatest amplitude of the interferometer with that of the encoder. However, due to the inconsistency of a data set within itself, this did not prove to be the most effective. A solution was to iterate around a certain range, which in this case was 0.94-1.06, by increments of 0.005. After further analyzing the data we concluded that another possible source of error was the inconsistency in period length, specifically, the period of one data set was longer than the other. The solution was to adjust the time span of the

interferometer data such that it matches the encoder data. This was done by changing the interferometer time step while iterating over the range of 5900-6100 with increments of 1. An additional step in data processing was to increase the number of data points. This was done first by decreasing the time step of the user-defined encoder time vector by a factor of 5, then interpolating the encoder position data with the time vector, then interpolating the interferometer position data as well. **Figure 5** shows an example of plot of a segment of data and the result of post processing.

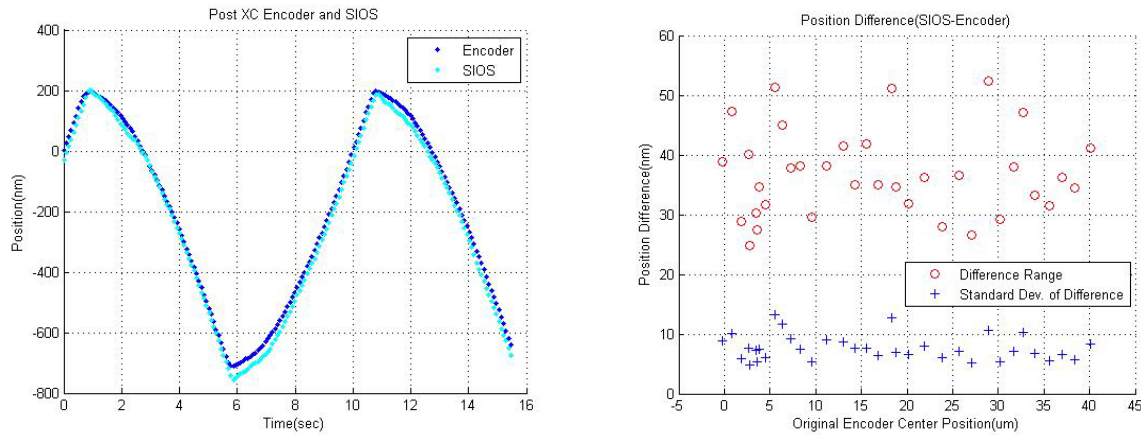


Figure 5: Post cross correlation and fined tuned data sample (left) and the difference range and standard deviation after post processing.

As a result of the increased number of data points and the use of smaller time step, the average range of difference was lowered to 36.72nm and the standard deviation was 7.65nm for the “thru-air” data and the average range of difference was lowered to 42.32nm and the standard deviation was 8.73nm for the “thru-water”.

The consistency within one set of data (either obtained by the encoder or the interferometer) itself was also investigated. The consistency of the encoder and interferometer was checked by cutting out two periods from the collected data, plotting them with the same time vector, and subtracting one from another to obtain the difference. The way the two segments were mapped onto each other was determined by cross correlation. It was found that in air, the average encoder discrepancy was 22.78nm with a standard deviation of 3.99nm while the interferometer discrepancy was 28.78nm with a 6.66nm standard deviation. Thru water, the average encoder discrepancy was 31.33nm and the standard deviation was 6.12nm while the interferometer discrepancy was 44.20nm and the standard deviation was 10.39nm.

5.0 Stability of the encoder- floating plate assembly in air

After assembling the sensor we performed a stability test in air. The sensor was placed on an optical table without any additional vibration isolation measures in a room where the temperature was not controlled. Encoder readings were recorded over two periods of time of approximately 4500 seconds. The first set of data started approximately 5 minutes after placing the encoder on the optical table. We observed that the encoder reading shifted to negative numbers and became stable after approximately 1 hour. No room or encoder temperature was measured.

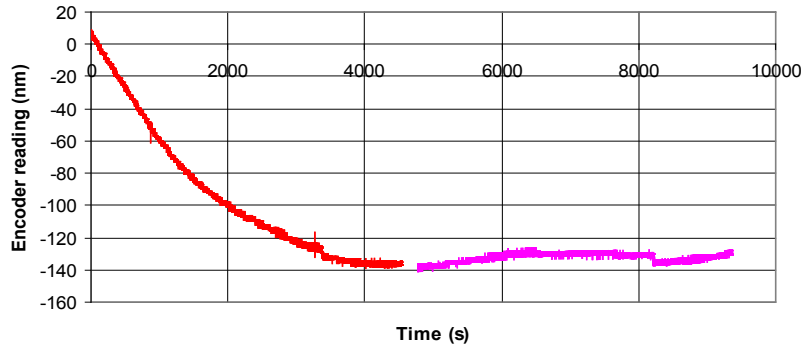


Figure 6: Stability test of the sensor assembly

6.0 Summary

A study is underway to develop a sensor array for measuring the flow fields and boundary erosion that are associated with scour at bridge piers. The focus of the report study has been on the individual sensor element and its ability to measure the shear force using a small sensor system. A 2D element was designed and fabricated using EDM and the requirements for the sensor to perform high accuracy measurements were investigated while addressing the related challenges.

7.0 Acknowledgement

The research reported herein was conducted at the Jet Propulsion Laboratory (JPL), California Institute of Technology, under a contract with the National Aeronautics and Space Administration (NASA). This JPL Task Plan No. 82-13107 was conducted under a contract with the Federal Highway Administration, Dept. of Transportation entitled "Flexible skin areal shear stress and pressure sensing system for experimental bridge scour research,"

8.0 References

- Akasofu K.-I., and M. R. Neuman, "A Thin-Film Variable Capacitance Shear Force Sensor for Medical and Robotics Applications," *Biosensors*, 9.4-3, 1991, pp. 1601-1602.
- Große S., W. Schroder and C. Brucker, "Nano-newton drag sensor based on flexible micro-pillars," *Measurement Science and Technology*, Institute of Physics Publishing Measurement Science and Technology, 17 (2006) 2689–2697 doi:10.1088/0957-0233/17/10/023
- Li, Y., Chandrasekharan, V., Bertolucci, B., Nishida, T., Cattafesta, L., and Sheplak, M., "A MEMS Shear Stress Sensor for Turbulence Measurements," *Proceedings of the 46th AIAA Aerospace Sciences Meeting and Exhibit*, AIAA 2008-269, Reno, Nevada, (7 - 10 January 2008)
- Naughton J.W. and M. Sheplak, "Modern developments in shear stress measurement", *Progress in Aerospace Sciences*, 38, pp. 515-570, 2002
- Qu Y., W. W. Y. Chow, Mengxing Ouyang, Steve C. H. Tung, Wen J. Li, and Xuliang Han, "Ultra-Low-Powered Aqueous Shear Stress Sensors Based on Integrated in Microfluidic Systems," *IEEE Transactions on Nanotechnology*, Vol. 7, No. 5, Sept. 2008 565
- Roche D., C. Richard, L. Eyraud, P. Gonnard, and C. Audoly, "A Piezoelectric Sensor Performing Shear Stress Measurement in an Hydrodynamic Flow," *ISAF 96 (International symposium on the Application of Ferroelectrics)*, UFFC IEEE conference (1996) pp. , 273-276
- Tunga S., H. Rokadiaa, and W. J. Lib "A micro shear stress sensor based on laterally aligned carbon nanotubes," doi:10.1016/j.sna.2006.04.039, *Sensors and Actuators A: Physical*, Volume 133, Issue 2, 12 February 2007, Pages 431-438
- Yucel O., and W. H. Graf, "Wall Shear Measurement in Sand-Water Mixture Flows," *Journal of the Hydraulics Division*, Vol. 101, No. 7, July 1975, pp. 947-963